ISSN: 0975-8585

Research Journal of Pharmaceutical, Biological and Chemical Sciences

A Density Functional Study of the Relationships between Electronic Structure and Dopamine D_2 receptor binding affinity of a series of [4-(4-Carboxamidobutyl)]-1-arylpiperazines.

Juan S. Gómez-Jeria* and Javier Valdebenito-Gamboa.

Quantum Pharmacology Unit, Department of Chemistry, Faculty of Sciences, University of Chile. Las Palmeras 3425, Santiago 7800003, Chile.

ABSTRACT

An analysis of the relationships between electronic structure and dopamine D_2 receptor binding affinity was carried out for a series of [4-(4-carboxamidobutyl)]-1-arylpiperazines. Local atomic reactivity indices were obtained at the B3LYP/6-31G(d,p) level after full geometry optimization. A statistically significant equation relating several local atomic reactivity indices with the binding affinity was obtained. From the results, a partial 2D pharmacophore is built, containing several sites that can be used for substitution enhancing binding affinity. An important conclusion is that because the common skeleton hypothesis is producing once more excellent results, the results reported here must serve as a guide for correct docking procedures.

Keywords: Dopamine receptors, D_2 receptor, binding affinity, DFT, QSAR.

*Corresponding author

ISSN: 0975-8585

INTRODUCTION

Dopamine (3,4-dihydroxyphenethylamine, DA) is a molecule of the catecholamine and phenethylamine families. In the brain, dopamine functions as a neurotransmitter. DA exerts its effects by interacting with a class of G protein-coupled receptors called dopamine receptors (DAR). Five DAR are known up to date; D_1, D_2, D_3, D_4 and D_5 [1, 2]. "*These functions include, but are not limited to, the following: voluntary movement, reward, sleep regulation, feeding, affect, attention, cognitive function, olfaction, vision, hormonal regulation, sympathetic regulation and penile erection. Dopamine receptors are also known to influence the immune system as well as cardiovascular, renal and gastrointestinal functions*" (taken from Ref. [1]). Multiple human disorders have been related to dopaminergic dysfunctions: attention deficit hyperactivity disorder, bipolar disorder, dyskinesias, drug addiction (and perhaps money, power and gambling addictions), Huntington's disease, hypertension, kidney dysfunction, major depression, Parkinson's disease, restless legs syndrome, schizophrenia and Tourette's syndrome. This area is the subject of actual intensive research [3-29]. As a result, many molecules interacting with DAR are employed for clinical use (see Table 3 of Ref. [1]). Also, many families of molecules interacting with one or more DAR have been synthesized and their biological activities measured and several theoretical studies have been carried out to understand the ligand-site interactions [30-48]. Here we present the results of a Density Functional Theory study of the relationships between electronic structure and D_2 receptor binding affinity for a family of [4-(4-carboxamidobutyl)]-1-arylpiperazines. A similar analysis of this same family but interacting with the D_3 receptor was reported elsewhere [49].

METHODS, MODELS AND CALCULATIONS

The QSAR method

Considering the method relating the electronic structure with the receptor binding affinity has been described in detail in several papers we present here the final equation in a standard form used en previous papers [50-55]. The receptor binding affinity (K_i) is related to a number of local atomic reactivity indices (LARIs) and has the following mathematical form:

$$\log(\mathrm{K}_i) = a + bM_{D_i} + c\log\left[\sigma_{D_i}/(ABC)^{1/2}\right] + \sum_j \left[e_j Q_j + f_j S_j^E + s_j S_j^N\right] +$$
$$+ \sum_j \sum_m \left[h_j(m)F_j(m) + x_j(m)S_j^E(m)\right] + \sum_j \sum_{m'} \left[r_j(m')F_j(m') + t_j(m')S_j^N(m')\right] +$$
$$+ \sum_j \left[g_j\mu_j + k_j\eta_j + o_j\omega_j + z_j\varsigma_j + w_j Q_j^{\max}\right] \qquad (1)$$

where M is the drug's mass, σ its symmetry number and ABC the product of the drug's moments of inertia about the three principal axes of rotation. Q_j is the net charge of atom j, S_j^E and S_j^N are, respectively, the total atomic electrophilic and nucleophilic superdelocalizabilities of atom j, $F_{j,m}$ ($F_{j,m'}$) is the Fukui index (electron population) of the occupied (vacant) MO m (m') localized on atom j [56]. $S_j^E(m)$ is the atomic electrophilic superdelocalizability of MO m localized on atom j, etc. The total atomic electrophilic superdelocalizability of atom j corresponds to the sum over occupied MOs of the $S_j^E(m)$'s and the total atomic nucleophilic superdelocalizability of atom j is the sum over vacant MOs of the $S_j^N(m)$'s. μ_j is the local atomic electronic chemical potential of atom j, η_j is the local atomic hardness of atom j, ω_j is the local atomic electrophilicity of atom j, ς_j is the local atomic softness of atom j, and $Q_j^{\max}$ is the maximal amount of electronic charge that atom j may accept from another site. $HOMO_j$* refers to the highest occupied molecular orbital localized on atom j and $LUMO_j$* to the lowest empty MO localized on atom j [55].

Selection of the molecules and the biological activity

ISSN: 0975-8585

The molecules and their D_2 receptor binding affinity (K) were selected from a recent publication [37]. Figure 1 and Tables 1a and 1b show, respectively, the molecules and the logarithm of the D_2 binding affinity, $\log(K_i)$.

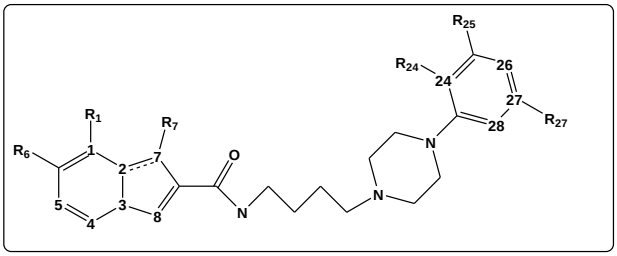

Figure 1. General structure of molecules.

Table 1a. Selected molecules.

Mol.	1	2	3	4	5	7	8	R_1	R_6	R_7
1	C	C	N	C	C	N	C	H	H	H
2	C	C	N	C	C	N	C	H	H	H
3	C	C	N	C	C	N	C	H	H	H
4	C	C	N	C	C	N	C	H	H	H
5	C	C	N	C	C	N	C	H	H	H
6	C	C	N	C	C	N	C	H	H	H
7	C	C	N	C	C	N	C	H	H	H
8	C	C	N	C	C	N	C	H	H	H
9	C	C	N	C	C	N	C	H	H	H
10	C	C	N	C	C	N	C	H	H	H
11	C	C	N	C	C	N	C	H	H	H
12	C	C	N	C	C	N	C	H	H	H
13	C	C	N	C	C	N	C	H	H	H
14	C	C	N	C	C	N	C	H	H	H
15	C	C	N	C	C	N	C	H	H	H
16	C	C	N	C	C	N	C	H	H	H
17	C	C	N	C	C	N	C	H	H	H
18	C	C	N	C	C	N	C	H	H	H
19	C	C	C	C	C	C	N	H	H	H
20	C	C	C	C	C	N	N	H	H	H
21	C	C	C	N	C	C	S	H	H	H
22	C	N	C	N	C	C	N	H	H	H
23	C	N	C	C	N	C	N	H	H	H
24	N	N	C	C	C	C	N	H	Cl	H
25	C	C	C	C	C	C	S	H	H	NH_2
26	C	C	C	C	C	C	C	H	H	$(CH_2)NMe_2$
27	C	N	C	C	C	C	N	H	H	$(CH_2)NMe_2$
28	C	N	C	C	C	C	N	$(CH_2)OH$	H	H
29	C	N	C	C	C	C	N	$(CH_2)NMe_2$	H	H

Table 1b. Selected molecules.

Mol.	26	28	R_{24}	R_{25}	R_{27}	R_{26}	$\log(K_i)$
1	C	C	H	H	H	H	2.25
2	C	C	OMe	H	H	H	1.28
3	C	C	Cl	Cl	H	H	1.08
4	C	C	CN	H	H	H	2.28
5	N	C	$(CH)_4$		H	H	2.76

6	N	C	$(CH)_4$		CF_3	H	4.13
7	C	C	$(CH)_2C(CF_3)(CH)$		H	H	3.70
8	N	C	$(CH)_2C(Cl)(CH)$		H	H	3.27
9	C	N	H	H	$(CH)_4$		3.19
10	N	N	$(CH)_4$		H	H	3.05
11	N	N	$(CH)_4$		t-Bu	H	3.16
12	N	N	H	CF_3	Me	H	4.40
13	N	N	H	Me	CF_3	H	3.54
14	N	N	H	t-Bu	Me	H	3.66
15	N	N	H	Me	t-Bu	H	2.56
16	N	N	H	t-Bu	t-Bu	H	2.56
17	N	N	H	c-Pr	t-Bu	H	2.28
18	N	N	H	CF_3	t-Bu	H	2.71
19	N	N	H	CF_3	t-Bu	H	2.96
20	N	N	H	CF_3	t-Bu	H	2.53
21	N	N	H	CF_3	t-Bu	H	2.83
22	N	N	H	CF_3	t-Bu	H	2.64
23	N	N	H	CF_3	t-Bu	H	2.65
24	N	N	H	CF_3	t-Bu	H	2.82
25	N	N	H	CF_3	t-Bu	H	2.68
26	N	N	H	CF_3	t-Bu	H	2.72
27	N	N	H	CF_3	t-Bu	H	2.48
28	N	N	H	CF_3	t-Bu	H	2.97
29	N	N	H	CF_3	t-Bu	H	2.47

Calculations

We employed the concept of common skeleton (a group of common atoms to all the molecules controlling almost all the variation of the receptor binding affinity through the variation of the numerical values of their LARIs). The common skeleton is shown in Fig. 2.

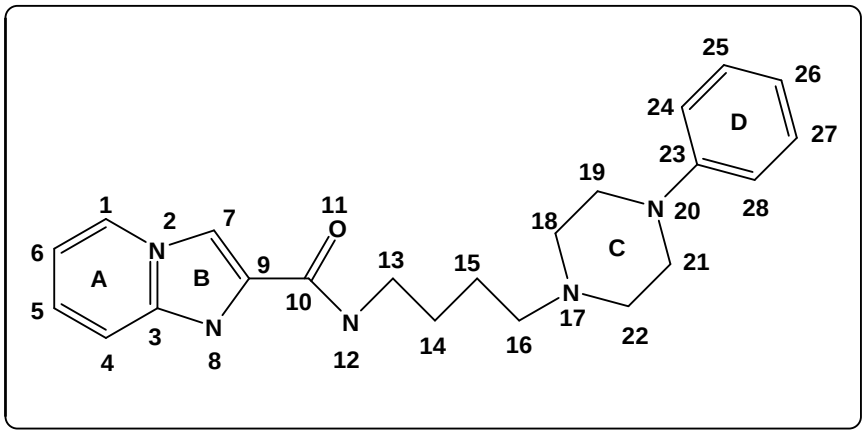

Figure 2. Common skeleton numbering.

All geometries were fully optimized at the DFT B3LYP/6-31G(d,p) level of theory with the Gaussian suite of programs [57]. From the log files of the single point calculations, we extracted all the necessary information to calculate the LARIs of the atoms composing the common skeleton with the D-Cent-QSAR software [58]. Mulliken Population Analysis results were corrected as usual [59]. Given that there are no enough binding affinity data to solve the linear system of Eqs. 1, we employed linear multiple regression analysis (LMRA) techniques to discover those indices whose variation explains the variation of the binding affinity. The Statistica software was used [60]. Here, statistics is employed as a slave.

ISSN: 0975-8585

RESULTS

No significant equation was obtained for the whole set of molecules (n=31) due to the presence of outliers. After eliminating them, the most statistically significant equation found is:

$$\log(K_i) = 3.66 + 5.85Q_{26}^{\max} + 0.20S_{25}^{E}(HOMO)^{*} + 0.02S_{2}^{N}(LUMO+1)^{*} + 1.34S_{21}^{N}(LUMO)^{*} - -0.56S_{7}^{E}(HOMO)^{*} - 0.36S_{9}^{E}(HOMO-1)^{*} + 4.69S_{15}^{N}(LUMO+1)^{*} + 0.63S_{4}^{E}(HOMO)^{*} - 0.38\mu_{18} - 0.54S_{18}^{E}(LUMO+1)^{*} \quad (2)$$

with n=28, R= 0.98, R^2= 0.97 adjusted R^2= 0.95, F(10,17)=53.817 (p<0.000001) and a standard error of estimate of 0.14. No outliers were detected and no residuals fall outside the ±2σ limits. Here, $Q_{26}^{\max}$ is the maximum amount of charge atom 26 may receive, $S_{25}^{E}(HOMO)^{*}$ is the electrophilic superdelocalizability of the highest occupied MO localized on atom 25, $S_{2}^{N}(LUMO+1)^{*}$ is the nucleophilic superdelocalizability of the second lowest vacant MO localized on atom 2, $S_{21}^{N}(LUMO)^{*}$ is the nucleophilic superdelocalizability of the lowest vacant MO localized on atom 21, $S_{7}^{E}(HOMO)^{*}$ is the electrophilic superdelocalizability of the highest occupied MO localized on atom 7, $S_{9}^{E}(HOMO-1)^{*}$ is the electrophilic superdelocalizability of the second highest occupied MO localized on atom 9, $S_{15}^{N}(LUMO+1)^{*}$ is the nucleophilic superdelocalizability of the second lowest vacant MO localized on atom 15, $S_{4}^{E}(HOMO)^{*}$ is the electrophilic superdelocalizability of the highest occupied MO localized on atom 4, μ_{18} is the local atomic electronic chemical potential of atom 18 and $S_{18}^{E}(LUMO+1)^{*}$ is the electrophilic superdelocalizability of the second lowest vacant MO localized on atom 18. Tables 2 and 3 show, respectively, the beta coefficients, the *t*-test for significance of the coefficients and the matrix of the squared correlation coefficients for the variables appearing in Eq. 2.

Table 2. Beta coefficients and *t*-test for significance of the coefficients in Eq. 2.

	Beta	B	t(17)	p-level
$Q_{26}^{\max}$	0.90	5.85	18.10	<0.000001
$S_{25}^{E}(HOMO)^{*}$	0.14	0.20	2.49	<0.02
$S_{2}^{N}(LUMO+1)^{*}$	0.42	0.02	6.67	<0.000004
$S_{21}^{N}(LUMO)^{*}$	0.83	1.34	11.48	<0.000001
$S_{7}^{E}(HOMO)^{*}$	-0.46	-0.56	-6.03	<0.00001
$S_{9}^{E}(HOMO-1)^{*}$	-0.19	-0.36	-2.88	<0.01
$S_{15}^{N}(LUMO+1)^{*}$	0.32	4.69	5.56	<0.00003
$S_{4}^{E}(HOMO)^{*}$	0.29	0.63	4.10	<0.0007
μ_{18}	-0.21	-0.38	-3.67	<0.002
$S_{18}^{E}(LUMO+1)^{*}$	-0.12	-0.54	-2.30	<0.03

We must note that in Table 2 there are three variables having a relatively high p-level.

ISSN: 0975-8585

Table 3. Matrix of squared correlation coefficients for the variables appearing in Eq. 2.

	Q_{26}^{max}	$S_{25}^{E}(HOMO)*$	$S_{2}^{N}(LUMO+1)*$	$S_{21}^{N}(LUMO)*$	$S_{7}^{E}(HOMO)*$	$S_{9}^{E}(HOMO-1)*$	$S_{15}^{N}(LUMO+1)*$	$S_{4}^{E}(HOMO)*$	μ_{18}
$S_{25}^{E}(HOMO)*$	0.04	1.00							
$S_{2}^{N}(LUMO+1)*$	0.01	0.06	1.00						
$S_{21}^{N}(LUMO)*$	0.21	0.09	0.02	1.00					
$S_{7}^{E}(HOMO)*$	0.005	0.09	0.21	0.05	1.00				
$S_{9}^{E}(HOMO-1)*$	0.01	0.004	0.20	0.10	0.10	1.00			
$S_{15}^{N}(LUMO+1)*$	0.03	0.03	0.001	0.16	0.004	0.04	1.00		
$S_{4}^{E}(HOMO)*$	0.001	0.02	0.07	0.08	0.16	0.12	0.02	1.00	
μ_{18}	0.0004	0.01	0.0004	0.09	0.10	0.16	0.03	0.23	1.00
$S_{18}^{E}(LUMO+1)*$	0.0004	0.002	0.03	0.13	0.06	0.07	0.005	0.11	0.16

Table 3 shows that no very significant internal correlations exist between the independent variables. The associated statistical parameters of Eq. 2 (Table 2) show that this equation is statistically significant and that the variation of a group of ten local atomic reactivity indices belonging to the common skeleton (Fig. 2) explains about 95% of the variation of log(K_i). Figure 3, spanning about 3 orders of magnitude, shows that there is a good quality correlation of observed *versus* calculated values and that very few points are far outside the 95% confidence interval.

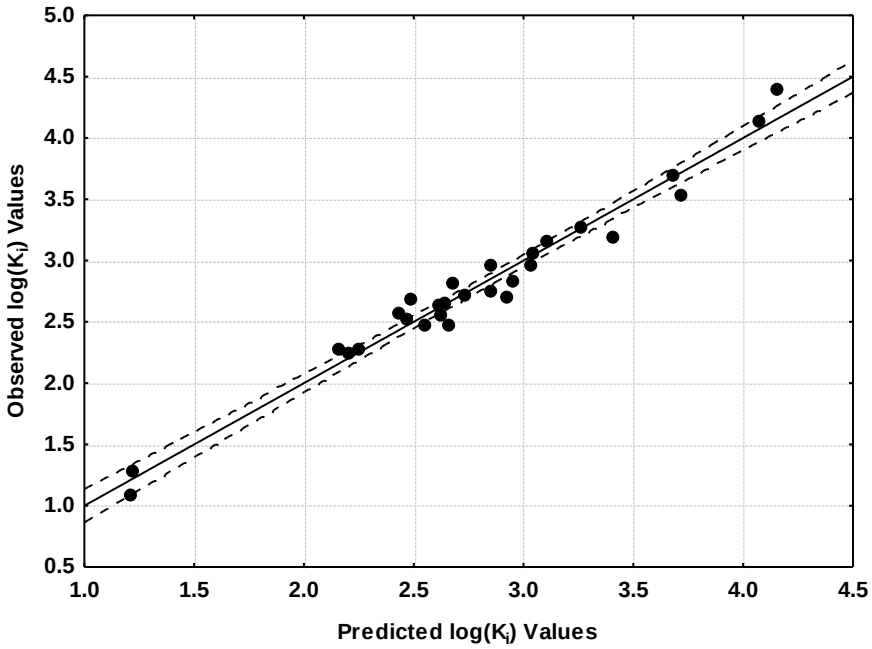

Figure 3. Plot of predicted *vs.* observed log(K_i) values from Eq. 2. Dashed lines denote the 95% confidence interval.

Tables 4 and 5 show the local molecular orbital structure of some atoms appearing in Eq. 2 (nomenclature: molecule (HOMO) / (HOMO-2)* (HOMO-1)* (HOMO)*-(LUMO)* (LUMO+1)* (LUMO+2)*).

ISSN: 0975-8585

Table 4. Local molecular orbital structure of atoms 2, 4, 7 and 9.

Mol	Atom 2 (C)	Atom 4 (C-N)	Atom 7 (C)	Atom 9 (C)
1 (101)	96π97π99π-103π105π110π	96π97π99π-102π105π108π	96π97π99π-102π103π105π	96π97π99π-102π103π105π
2 (109)	104π105π107π-111π114π117π	103π104π107π-110π114π115π	104π105π107π-110π111π114π	104π105σ107π-110π111π114π
3 (117)	113π115π116π-119π123π128π	113π115π116π-118π123π126π	113π115π116π-118π119π123π	113π115π116π-118π119π123π
4 (123)	119π120π122π-127π128π135π	118π119π122π-125π128π132π	119π120π122π-125π127π128π	119π120π122π-125π127π128π
5 (114)|	107π108π112π-117π119π127π	107π108π112π-115π119π122π	107π108π112π-115π117π119π	107π108π112π-115π117π119π
6 (130)	126π127π128π-134π135π143π	122π125π128π-132π135π139π	126π127π128π-132π134π135π	126π127σ128π-132π134π135π
7 (130)	124π127π128π-134π135π143π	124π127π128π-131π134π135π	124π127π128π-131π134π135π	124π127σ128π-131π134π135π
8 (122)	116π117π120π-125π127π134π	116π117π120-123π125π127π	116π117π120π-123π125π127π	116π117π120-123π125π127π
9 (114)	108π109π112π-117π119π124π	108π109π112π-115π119π122π	108π109π112π-115π117π119π	108π109π112π-115π117π119π
10 (114)	109π110π112π-117π119π125π	109π110π112π-115π119π122π	109π110π112π-115π117π119π	109π110π112π-115π117π119π
11 (130)	125π126π128π-133π135π141π	125π126π128π-131π135π138π	125π126π128π-131π133π135π	125π126π128π-131π133π135π
12 (121)	116π117π120π-124π126π130π	116π117π120π-122π126π128π	116π117π120π-122π124π126π	117π118π120π-122π124π126π
13 (121)	116π118π120π-124π126π132π	116π118π120π-122π126π128π	116π118π120π-122π124π126π	116π118π120π-122π124π126π
14 (121)	116π117π119π-123π126π131π	116π117π119π-122π126π128π	116π117π119π-122π123π126π	116π117π119π-122π123π126π
15 (121)	116π117π119π-123π126π130π	116π117π119π-122π126π128π	116π117π119π-122π123π126π	116π117π119π-122π123π126π
16 (133)	128π129π131π-135π138π143π	128π129π131π-134π138π140π	128π129π131π-134π135π138π	128π129π131π-134π135π138π
17 (128)	122π124π126π-130π133π138π	121π122π126π-129π133π135π	122π124π126π-129π130π133π	122π124π126π-129π130π133π
18 (133)	128π129π132π-136π138π142π	127π128π132π-134π138π140π	128π129π132π-134π136π138π	129π130π132π-134π136π138π
19 (133)	130π131π132π-134π137π138π	130π131π132π-134π137π138π	124π130π132π-134π137π138π	130π131π132π-134π137π138π
20 (133)	128σ130π131π-134π137π138π	126σ130π131π-134π137π138π	128σ130π131π-134π137π138π	128σ130π131π-134π137π138π
21 (137)	132π133π135π-138π140π142π	132π133π135π-138π140π142π	132π133π135π-138π140π142π	132π133π135π-138π140π142π
22 (133)	125σ127π129π-134π136π138π	125σ127π131π-134π136π138π	128σ129π131π-136π138π140π	128σ129π131π-134π136π138π
23 (133)	126σ127π131π-134π136π138π	126σ127π131π-134π138π143π	128σ129π131π-136π138π140π	128σ129π131π-134π136π138π
24 (141)	132σ135π137π-142π143π146π	132σ135π138π-142π143π146π	136σ137π138π-143π145π146π	136σ137π138π-142π143π145π
25 (141)	136π137π140π-142π144π146π	135σ137π140π-142π144π147π	134σ135π140π-142π144π146π	136π137π140π-142π144π146π
26 (149)	141π146π147π-150π153π154π	146π147π149π-150π153π154π	146π147π149π-150π154π155π	146π147π149π-150π153π154π

27 (145)	141π143π144π-146π148π150π	138π141π144π-146π148π150π	141π143π144π-146π148π150π	141π143σ144π-146π148π150π
28 (141)	132σ135π138π-142π144π146π	135π138π140π-142π144π146π	136σ138π140π-142π144π146π	136σ138π140π-142π144π146π
29 (149)	142π145π148π-150π152π154π	142π145π148π-150π152π154π	145π146π148π-152π154π157π	144σ145π148π-150π152π154π

Table 5. Local molecular orbital structure of atoms 15, 18, 21 and 25.

Mol	Atom 15 (C)	Atom 18 (C)	Atom 21 (C)	Atom 25 (C)
1 (101)	96σ100σ101σ-116σ120σ121σ	94σ100σ101σ-110σ115σ117σ	94σ100σ101σ-111σ113σ114σ	94π98π101π-104π106π111π
2 (109)	104σ108σ109σ-122σ125σ128σ	102σ108σ109σ-116σ121σ122σ	106σ108σ109σ-118σ122σ124σ	102π106π108π-112π113π118π
3 (117)	112σ116σ117σ-130σ137σ138σ	110σ116σ117σ-121σ129σ131σ	115σ116σ117σ-129σ133σ135σ	108σ110π114π-120π121π122π
4 (123)	114σ119σ123σ-136σ139σ140σ	117σ121σ123σ-139σ142σ143σ	117σ121σ123σ-126σ129σ137σ	109σ110π115π-124π126π129π
5 (114)|	109σ113σ114σ-123σ130σ131σ	109σ113σ114σ-126σ129σ130σ	109σ113σ114σ-116σ120σ125σ	110σ111π113π-118π120π137π
6 (130)	122σ129σ130σ-138σ141σ144σ	126σ129σ130σ-136σ140σ142σ	120σ126σ130σ-137σ144σ145σ	125π126π130π-133π136π141π
7 (130)	124σ129σ130σ-145σ147σ150σ	123σ129σ130σ-142σ143σ144σ	123σ129σ130σ-132σ136σ139σ	124π125π126π-132π133π136π
8 (122)	116σ121σ122σ-132σ138σ139σ	115σ121σ122σ-134σ135σ136σ	115σ121σ122σ-124σ128σ133σ	116π118σ119π-126π128π129π
9 (114)	108σ113σ114σ-126σ130σ131σ	106σ113σ114σ-127σ129σ130σ	106σ113σ114σ-125σ126σ127σ	106π111π113π-116π120π125π
10 (114)	109σ113σ114σ-129σ133σ134σ	106σ108σ114σ-128σ129σ130σ	108σ113σ114σ-116σ120σ124σ	111σ113π114π-116π118π120π
11 (130)	125σ129σ130σ-144σ146σ150σ	124σ129σ130σ-145σ146σ147σ	124σ129σ130σ-132σ136σ142σ	127σ129π130π-132π134π136π
12 (121)	116σ119σ121σ-133σ136σ139σ	111σ119σ121σ-130σ132σ133σ	113σ119σ121σ-131σ134σ135σ	113π118σ119π-123π125π131π
13 (121)	116σ119σ121σ-133σ137σ139σ	111σ119σ121σ-130σ132σ133σ	112σ119σ121σ-131σ132σ133σ	113σ117σ119π-123π125π135π
14 (121)	116σ120σ121σ-132σ134σ136σ	111σ120σ121σ-135σ137σ138σ	114σ120σ121σ-130σ133σ134σ	118σ120π121π-124π125π137π
15 (121)	116σ120σ121σ-139σ140σ142σ	111σ120σ121σ-130σ134σ136σ	111σ120σ121σ-131σ133σ134σ	114π118σ120π-124π136π139π
16 (133)	128σ132σ133σ-145σ148σ149σ	123σ132σ133σ-147σ148σ150σ	126σ132σ133σ-146σ148σ149σ	130σ132π133π-136π137π150π
17 (128)	122σ127σ128σ-142σ148σ149σ	115σ127σ128σ-141σ142σ143σ	118σ127σ128σ-137σ141σ142σ	125σ127π128π-131π139π145π
18 (133)	128σ131σ133σ-145σ149σ151σ	121σ131σ133σ-144σ145σ148σ	125σ131σ133σ-143σ144σ147σ	125π130σ131π-135π137π143π
19 (133)	121σ128σ133σ-141σ145σ149σ	120σ121σ133σ-144σ145σ146σ	130σ131σ133σ-142σ143σ144σ	125σ126π129σ-135π136π148π
20 (133)	120σ132σ133σ-142σ146σ149σ	120σ132σ133σ-145σ146σ148σ	125σ132σ133σ-144σ145σ148σ	125π129σ132π-135π136π148π
21 (137)	124σ136σ137σ-154σ155σ156σ	124σ136σ137σ-149σ150σ153σ	129σ136σ137σ-147σ148σ149σ	129π134σ136π-139π141π152π
22 (133)	129σ132σ133σ-142σ150σ151σ	120σ132σ133σ-142σ143σ144σ	126σ132σ133σ-141σ143σ146σ	126π130σ132π-135π137π149π
23 (133)	129σ132σ133σ-	120σ132σ133σ-	125σ132σ133σ-	125π130σ132π-

	150σ151σ152σ	142σ143σ149σ	142σ143σ144σ	135π137π149π
24 (141)	137σ140σ141σ-158σ159σ160σ	129σ140σ141σ-154σ157σ159σ	134σ140σ141σ-151σ152σ153σ	134π139σ140π-144π157π159π
25 (141)	128σ139σ141σ-159σ161σ162σ	128σ139σ141σ-151σ153σ154σ	133σ139σ141σ-152σ153σ155σ	133π138σ139π-143π145π157π
26 (149)	136σ145σ148σ-158σ160σ166σ	136σ145σ148σ-160σ161σ163σ	140σ145σ148σ-159σ161σ165σ	140π144σ145π-151π152π165π
27 (145)	141σ142σ145σ-162σ165σ166σ	132σ142σ145σ-155σ157σ160σ	137σ142σ145σ-153σ155σ156σ	137π140σ142π-147π149π160π
28 (141)	138σ139σ141σ-152σ159σ160σ	129σ139σ141σ-152σ154σ158σ	134σ139σ141σ-150σ153σ155σ	134π137σ139π-143π145π154π
29 (149)	145σ147σ149σ-159σ167σ172σ	138σ147σ149σ-159σ161σ165σ	141σ147σ149σ-158σ160σ163σ	141π143σ147π-151π153π161π

DISCUSSION

We shall employ the variable-by-variable analysis. Note that this kind of analysis is approximate because the variation of the receptor binding affinity is related to the simultaneous variation of all the LARIs appearing in Eq. 2. The beta values (Table 2) show that the importance of variables is $Q_{26}^{\max}$ > $S_{21}^{N}(LUMO)*$ >> $S_{7}^{E}(HOMO)*$ > $S_{2}^{N}(LUMO+1)*$ > $S_{15}^{N}(LUMO+1)*$ > $S_{4}^{E}(HOMO)*$ > μ_{18} > $S_{9}^{E}(HOMO-1)*$ > $S_{25}^{E}(HOMO)*$ > $S_{18}^{E}(LUMO+1)*$. Eq. 2 shows that a high receptor binding affinity is associated with high numerical values for $\left|S_{25}^{E}(HOMO)*\right|$, $\left|S_{4}^{E}(HOMO)*\right|$ and $\left|\mu_{18}\right|$, and with low numerical values for $Q_{26}^{\max}$, $\left|S_{7}^{E}(HOMO)*\right|$, $\left|S_{9}^{E}(HOMO-1)*\right|$ and $\left|S_{18}^{E}(LUMO+1)*\right|$. If $S_{21}^{N}(LUMO)*$ is positive, a small numerical value is associated with high affinity. If $S_{15}^{N}(LUMO+1)*$ is positive, a small numerical value is associated with high affinity. If $S_{2}^{N}(LUMO+1)*$ is positive, a small numerical value is associated with high affinity. Atom 26 is a carbon in the aromatic ring D (Fig. 2). A high value for $Q_{26}^{\max}$ suggests that this atom is interacting with an electron-rich center. Concerning that atom 26 has a negative net charge, it could be engaged in π-π or π-σ (π-alkyl) interactions. The fact that atom 25 is also involved (see below) suggests that the most probable interaction is a π-π one (stacked or T-shaped). Atom 21 is a carbon in the saturated ring C (Fig. 2). All MOs are of σ nature. The numerical values of $S_{21}^{N}(LUMO)*$ are positive in some molecules and negative in others. For the positive case small values are needed, and for the negative case high negative values are optimal. In both cases, the associated eigenvalue of $(LUMO)_{21}^{*}$ should be shifted upwards in the energy axis, producing a less reactive MO. Therefore, we suggest that atom 21 is interacting with an electron-deficient center having several vacant MOs that can engage in a repulsive interaction with $(LUMO)_{21}^{*}$. Possible interactions are carbon H-bond (C21-H...π), σ-σ or σ-π ones. Atom 7 is a carbon in aromatic ring B (Fig. 2). A low value for $\left|S_{7}^{E}(HOMO)*\right|$ can be obtained by shifting downwards the HOMO energy and/or by diminishing the value of $F_{7}(HOMO)*$ (this index has a non-zero value by definition, see [55]). This MO has a π nature (Table 4). The necessity of a less reactive MO suggests that atom 7 is interacting with an electron-rich center. Possible interactions: π-π, C-H bond and π-anion. Atom 2 is a carbon belonging to aromatic rings A and B (Fig. 2). $(LUMO+1)_{2}^{*}$ has a π nature (Table 4). A high binding affinity is associated with small (positive) numerical values if $S_{2}^{N}(LUMO+1)*$ is positive and with high (negative) numerical values if $S_{2}^{N}(LUMO+1)*$ is negative. Our results show that in some cases the numerical value of $S_{2}^{N}(LUMO+1)*$ is positive, and that in others is negative. Let us consider the positive case, where a small numerical value is required. This small value is obtained by shifting upwards the $(LUMO+1)_{2}^{*}$ eigenvalue, producing a less reactive MO. If $S_{2}^{N}(LUMO+1)*$ is negative, high negative

values of $S_2^N(LUMO+1)*$ are obtained again by shifting upwards the $(LUMO+1)_2^*$ eigenvalue, producing again a less reactive MO. A possible explanation of this requirement is that $(LUMO)_2^*$ is interacting with an electron-rich counterpart and that $(LUMO+1)_2^*$ is engaged in repulsive interactions with the vacant MOs of this moiety [61, 62]. Possible interactions: π-π and π-anion. Atom 15 is a carbon of a methylene chain joining rings B and C (Fig. 2). All local MOs are of σ nature (Table 5). Our results indicate that the numerical values of $S_{15}^N(LUMO+1)*$ are positive in all molecules. A high binding affinity is associated with low positive numerical values for this index. Employing the same analysis used for $S_2^N(LUMO+1)*$ we suggest that the σ electrons of $(LUMO+1)_{15}^*$ are engaged in a repulsive interaction with vacant MOs of a moiety, while $(LUMO)_{15}^*$ is interacting with an electron-rich center. Possible interactions: C-H…π, σ-σ and σ-π. Atom 4 is a carbon in aromatic ring A (Fig. 2). High negative values of $S_4^E(HOMO)*$ are associated with high binding affinity. $(HOMO)_4^*$ is of π nature (Table 4). It is suggested that atom 4 is interacting with an electron-deficient center. Possible interactions: π-π, C-H bond and π-cation. Atom 18 is a carbon of the saturated ring C (Fig. 2). All MOs are of σ nature (Table 5). A low (negative) numerical value for $S_{18}^E(HOMO-1)*$ is optimal for high binding affinity, indicating that $(HOMO-1)_{18}^*$ could be interacting in an unfavorable way with one or more occupied MOs of a moiety in the binding site. Regarding $(HOMO)_{18}^*$, it could be engaged in an interaction with only the lowest vacant MO localized on the moiety. On the other hand, a high affinity is also associated with low negative numerical values for the local atomic electronic chemical potential, μ_{18}. This local atomic index is the midpoint between $(HOMO)_{18}^*$ and $(LUMO)_{18}^*$, and low negative values can be obtained by shifting upwards the $(HOMO)_{18}^*$ energy. This will augment the $(HOMO)_{18}^*$-$(HOMO-1)_{18}^*$ gap, fact that is not in contradiction with the requirements for $(HOMO-1)_{18}^*$. Possible interactions: C-H…π, σ-σ and σ-π. Atom 9 is a carbon of aromatic ring B (Fig. 2). $(HOMO)_9^*$ and $(HOMO-1)_9^*$ have π nature (Table 4). A high affinity is associated with low negative numerical values for $S_9^E(HOMO-1)*$. This fact suggests that $(HOMO-1)_9^*$ could be engaged in unfavorable interactions with occupied MOs of the site. As in the case of atom 18, $(HOMO)_9^*$ seems to interact with the lowest local empty MO of a residue. Possible interaction: π-π. Atom 25 is a carbon of the aromatic ring D (Fig. 2). A high negative numerical value for $S_{25}^E(HOMO)*$ is associated with high binding affinity. $(HOMO)_{25}^*$ has a π nature (Table 5). Therefore, atom 25 is interacting with an electron-deficient center through its highest occupied local MO. Possible interactions: π-π or π-σ (π-alkyl), being the π-π (T-shaped or stacked) the most probable one. All the aforementioned suggestions are summarized in the two dimensional (2D) partial pharmacophore shown in Fig. 4.

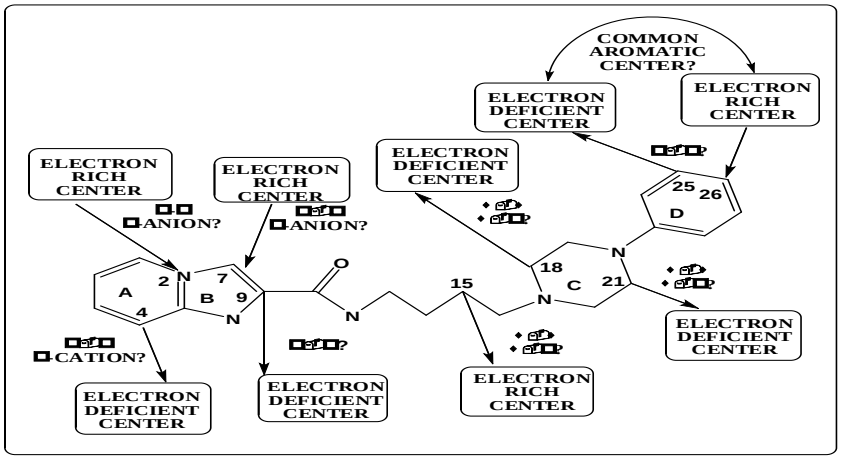

Figure 4. Partial 2D pharmacophore for D2 receptor binding affinity.

ISSN: 0975-8585

This pharmacophore contains several atoms that can be employed as targets for testing substitutions enhancing the D_2 receptor binding affinity.

Conformational freedom

The partial pharmacophore is always shown as a 2D figure because our method is not able to provide three-dimensional information about the interactions. Theoretically the results presented here can be supported by docking analysis with a model of the D2 receptor. As the results presented here sustain the hypothesis of the existence of a common skeleton (Fig. 2) aligned in a similar way during the drug-receptor interaction, a good docking study should produce results supporting this fact. The molecules studied here have a high degree of conformational flexibility due to the long chain joining rings B and C. As an example, figure 5 shows the ten lowest energy conformers of molecules 5 and 17 obtained with MarvinView and superimposed with Hyperchem (atoms 4, 6 and 7 of rings A and B of Fig. 2 were employed as the common elements for superimposition) [63, 64].

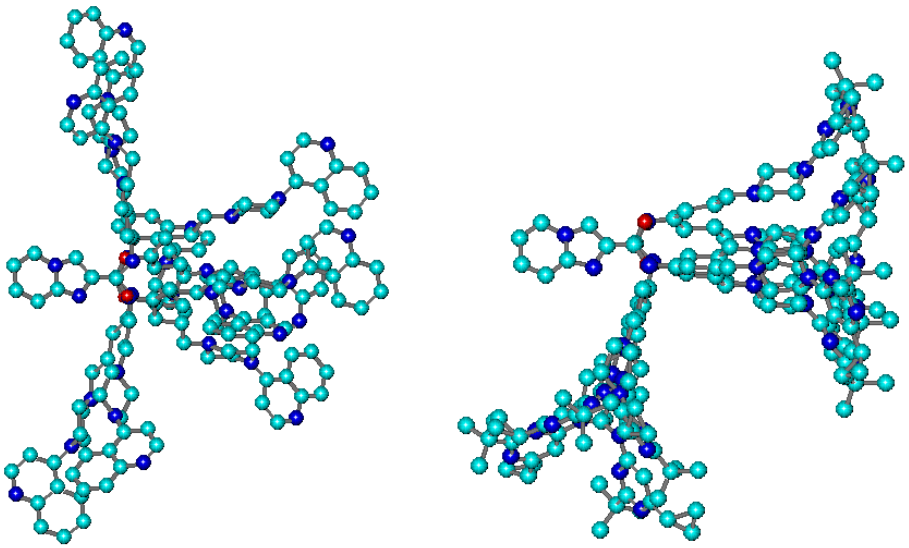

Figure 5. Superimposition of the ten lowest energy conformers of molecules 5 (left) and 17 (right).

We can observe that both molecules have a high degree of conformational flexibility. The unknown microscopic environment existing around the binding site at the moment of the interaction will select one of these conformers as the active one. Figure 6 shows the superimposition of the common skeleton of the 29 molecules analyzed here using the DFT fully optimized geometries.

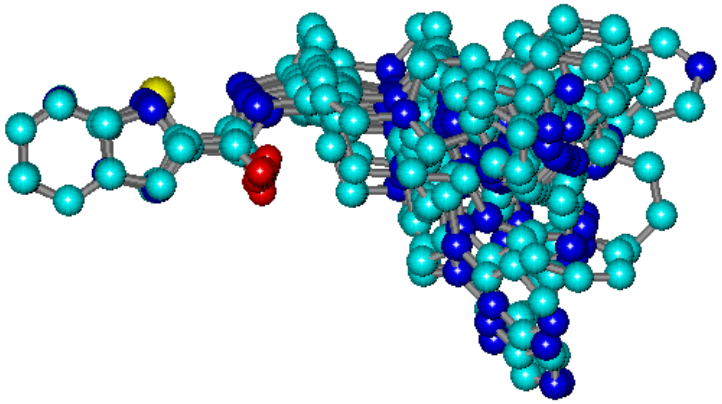

Figure 6. Superimposition of the common skeleton of molecules 1-29.

We can see that, if all the consequences of the common skeleton hypothesis are true, then several or all the molecules must change their conformation to adapt themselves to an unknown common conformation. As in one-step processes (i.e., receptor binding affinities) the common skeleton hypothesis provided excellent results beyond a reasonable doubt, we suggest that it should be taken as a starting point for docking studies [49, 65-88]. We are actually trying to develop a methodology making docking studies compatible with the kind of formal results obtained here.

Molecular Electrostatic Potential (MEP)

MEP maps can provide a first insight about the probable orientation of the molecules while they approach the binding site. Figure 7 displays the MEP maps of molecules 5 and 17 in their fully optimized geometry.

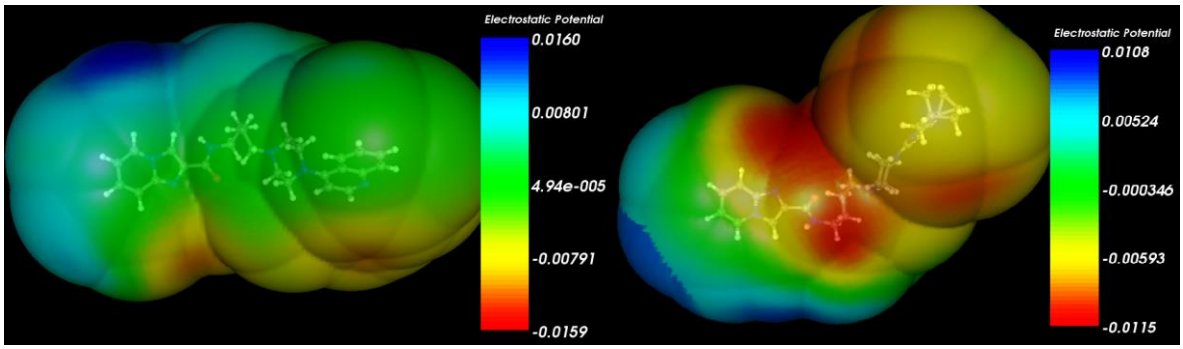

Figure 7. MEP map of molecules 5 (left) and 17 (right) at 5 Å of the nuclei.

Let us accept as a working hypothesis that at a distance of 5 Å from the receptor the conformations of molecules 5 and 17 are the ones represented in Fig. 7. If this is true then we can observe that at the left side of both molecules there is a similar region of positive electrostatic potential. Then the ring A-B system could be the side pointing to the receptor. Unhappily, this is not necessarily true because at least we do not know if these conformations actually exist at 5 Å and we do not know in addition the composition of the microscopic milieu at that distance and how it affects the conformations. Therefore, these kinds of representations have only a limited value and must be used carefully. Figure 8 shows the MEP map of molecules 7 and 17 at the ±0.0004 isovalue, using the fully optimized geometries.

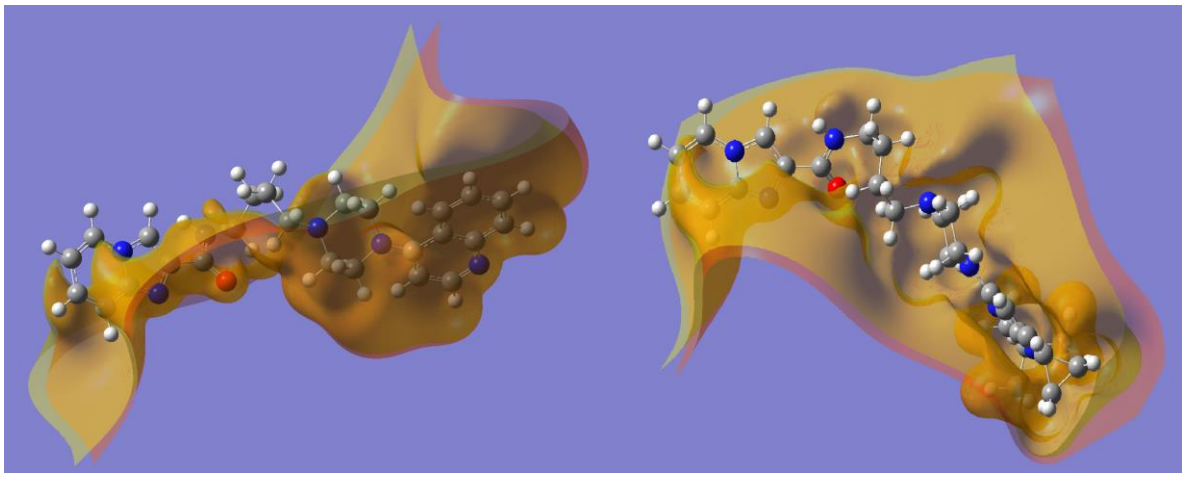

Figure 8. Molecular electrostatic potential map of molecules 7 (left) and 17 (right). The orange isovalue surface corresponds to a negative MEP value (-0.0004) and the yellow isovalue surface to a positive MEP value (0.0004).

We can observe the existence of a positive MEP region covering the upper parts of rings A and B, the upper part of the chain linking rings B and C and the upper parts of rings C and D. This distribution of positive

potential values seems to be independent of the conformation of rings C and D. This statement can be confirmed only by a study of the MEP at several different conformations. Anyway if we still accept that these molecules approach the site with ring A pointing to it, then the molecules should be facing a volume having a negative electrostatic potential.

Local Molecular Orbitals

Here we shall present two examples to help to understand the concept of local molecular orbitals. Figure 9 shows the HOMO of molecules 26 and 29.

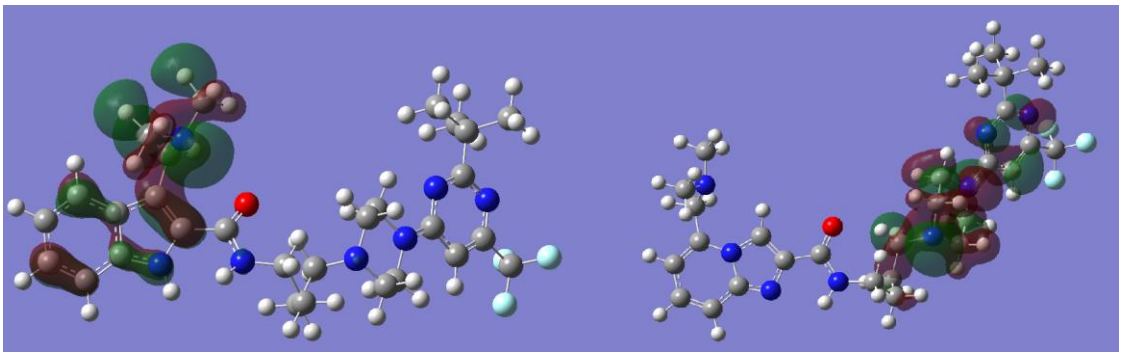

Figure 9. HOMO of molecules 26 (left) and 29 (right).

An important point to comment on is that the size of the molecular orbitals depicted in the figure strongly depends on the value chosen for the isosurface. The smaller the value, the larger the MO. We can see that the HOMO of molecule 26 is localized on part of ring A, ring B and the substituent. For this reason we may state that for the atoms on which the molecular HOMO is localized, this MO is their local HOMO (HOMO*). In the remaining of the molecule, where the molecular HOMO is not localized, the local HOMO* will be the highest occupied MO localized on these atoms (that can be the molecule's HOMO-1, HOMO-2, etc.). In the case of molecule 29, the molecular HOMO is localized on rings C and D. Therefore for these rings the molecule's HOMO is the local HOMO*. For the atoms of rings A and B we must find the highest occupied MO localized on them to find the corresponding HOMO*. Figure 10 shows the LUMO of molecules 1 and 4.

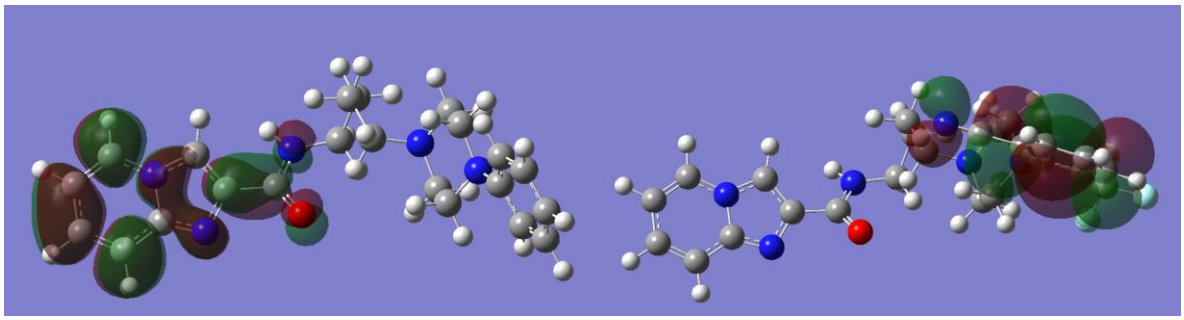

Figure 10. LUMO of molecules 1(left) and 4 (right).

We can see that the LUMO is localized on different rings of these molecules. For molecule 1, the LUMO* of several atoms of rings A and B is more or less coincident with the MO localized on them. For the remaining atoms their corresponding LUMO* will be the lowest vacant MO localized on them. Molecule 4 is another example. To become independent of the visual representations of the MOs we have proposed earlier that, for example, the HOMO* of a given atom will be the highest occupied MO in which the associated Fukui index (i.e., the electron population) of this atom be equal or greater than 0.01 etc.

CONCLUSIONS

We have obtained a statistically significant relationship between electronic structure and dopamine D_2 receptor binding affinity for a group of [4-(4-carboxamidobutyl)]-1-arylpiperazines. The corresponding 2D

pharmacophore and the possible ligand-site interactions are proposed. The conformational aspects of the molecules are discussed. As the common skeleton hypothesis works very well in this case, it is proposed that docking studies should be guided by the results obtained here.

REFERENCES

[1] Beaulieu, J-M, Espinoza, S, Gainetdinov, RR. Brit. J. Pharmacol., 2015, 172, 1-23.
[2] Beaulieu, J-M, Gainetdinov, RR. Pharmacol. Rev., 2011, 63, 182-217.
[3] Tolboom, N, Berendse, HW, Leysen, JE, Yaqub, M, van Berckel, BNM, Schuit, RC, Ponsen, MM, Bakker, E, Hoetjes, NJ, Windhorst, AD, Carlsson, ML, Lammertsma, AA, Carlsson, A. Neuropsychopharm., 2015, 40, 472-479.
[4] Smith, LN, Bachus, SE, McDonald, CG, Smith, RF. Behav. Brain. Res., 2015, 289, 92-104.
[5] Nutt, DJ, Lingford-Hughes, A, Erritzoe, D, Stokes, PRA. Nat. Rev. Neurosci., 2015, 16, 305-312.
[6] Min, C, Zheng, M, Zhang, X, Guo, S, Kwon, K-J, Shin, CY, Kim, H-S, Cheon, SH, Kim, K-M. Biochem. Bioph. Acta Mol. Cell. Res., 2015, 1853, 41-51.
[7] Martelle, S, Nader, SH, Czoty, PW, John, WS, Newman, AH, Nader, MA. Drug Alc. Dep., 2015, 146, e193-e194.
[8] Marsango, S, Caltabiano, G, Pou, C, Varela Liste, MJ, Milligan, G. J. Biol. Chem., 2015,
[9] Li, Y, Zhu, ZR, Ou, BC, Wang, YQ, Tan, ZB, Deng, CM, Gao, YY, Tang, M, So, JH, Mu, YL, Zhang, LQ. Behav. Brain. Res., 2015, 279, 100-105.
[10] Kota, K, Kuzhikandathil, EV, Afrasiabi, M, Lacy, B, Kontoyianni, M, Crider, AM, Song, D. Pharmacol. Res., 2015, 99, 174-184.
[11] Keck, TM, John, WS, Czoty, PW, Nader, MA, Newman, AH. J. Med. Chem., 2015,
[12] John, WS, Newman, AH, Nader, MA. Drug Alc. Dep., 2015, 146, e148-e149.
[13] Hounsou, C, Margathe, J-F, Oueslati, N, Belhocine, A, Dupuis, E, Thomas, C, Mann, A, Ilien, B, Rognan, D, Trinquet, E, Hibert, M, Pin, J-P, Bonnet, D, Durroux, T. ACS Chem. Biol., 2015, 10, 466-474.
[14] Franz, D, Contreras, F, González, H, Prado, C, Elgueta, D, Figueroa, C, Pacheco, R. J. Neuroimm., 2015, 284, 18-29.
[15] Foll, BL, Payer, D, Ciano, PD, Guranda, M, Nakajima, S, Tong, J, Mansouri, E, Wilson, AA, Houle, S, Meyer, JH, Graff-Guerrero, A, Boileau, I. Neuropsychopharm., 2015,
[16] Emery, MA, Bates, MLS, Wellman, PJ, Eitan, S. Behav. Brain. Res., 2015, 284, 37-41.
[17] Castro-Hernández, J, Afonso-Oramas, D, Cruz-Muros, I, Salas-Hernández, J, Barroso-Chinea, P, Moratalla, R, Millan, MJ, González-Hernández, T. Neurobiol. Dis., 2015, 74, 325-335.
[18] Ballard, ME, Mandelkern, MA, Monterosso, JR, Hsu, E, Robertson, CL, Ishibashi, K, Dean, AC, London, ED. Int J Neuropsychopharmacol., 2015, 18, pyu119.
[19] Abi-Jaoude, E, Segura, B, Obeso, I, Cho, SS, Houle, S, Lang, AE, Rusjan, P, Sandor, P, Strafella, AP. Human Brain Mapp., 2015, 36, 2592-2601.
[20] Yan, Y, Newman, AH, Xu, M. Neurosci., 2014, 278, 154-164.
[21] Ustione, A, Jacobson, DA, Piston, DW. Biophys. J., 2014, 106, 718a.
[22] Simpson, EH, Winiger, V, Biezonski, DK, Haq, I, Kandel, ER, Kellendonk, C. Biol. Psych., 2014, 76, 823-831.
[23] Shimizu, S, Tatara, A, Sato, M, Sugiuchi, T, Miyoshi, S, Andatsu, S, Kizu, T, Ohno, Y. Prog. Neuro-psychopharm. Biol. Psych., 2014, 50, 157-162.
[24] Neisewander, JL, Cheung, THC, Pentkowski, NS. Neuropharm., 2014, 76, Part B, 301-319.
[25] Moraga-Amaro, R, Gonzalez, H, Pacheco, R, Stehberg, J. Behav. Brain. Res., 2014, 274, 186-193.
[26] Matuskey, D, Gallezot, J-D, Pittman, B, Williams, W, Wanyiri, J, Gaiser, E, Lee, DE, Hannestad, J, Lim, K, Zheng, M-Q, Lin, S-f, Labaree, D, Potenza, MN, Carson, RE, Malison, RT, Ding, Y-S. Drug Alc. Dep., 2014, 139, 100-105.
[27] Eagle, DM, Noschang, C, d'Angelo, L-SC, Noble, CA, Day, JO, Dongelmans, ML, Theobald, DE, Mar, AC, Urcelay, GP, Morein-Zamir, S, Robbins, TW. Behav. Brain. Res., 2014, 264, 207-229.
[28] Cote, SR, Chitravanshi, VC, Bleickardt, C, Sapru, HN, Kuzhikandathil, EV. Behav. Brain. Res., 2014, 263, 46-50.
[29] Baladi, MG, Newman, AH, Nielsen, SM, Hanson, GR, Fleckenstein, AE. Eur. J. Pharmacol., 2014, 732, 105-110.
[30] Peng, X, Wang, Q, Mishra, Y, Xu, J, Reichert, DE, Malik, M, Taylor, M, Luedtke, RR, Mach, RH. Biorg. Med. Chem. Lett., 2015, 25, 519-523.

[31] Moritz, A, Free, R, Weiner, W, Bachani, M, Conroy, J, Barnaeva, E, Hu, X, Southall, N, Ferrer, M, Javitch, J, Steiner, J, Aube, J, Frankowski, K, Sibley, D. The FASEB Journal, 2015, 29,
[32] Michino, M, Shi, L, "Computational Approaches in the Structure–Function Studies of Dopamine Receptors," in *Dopamine Receptor Technologies*, M. Tiberi Ed., vol. 96, pp. 31-42, Springer New York, 2015.
[33] Keck, TM, Banala, AK, Slack, RD, Burzynski, C, Bonifazi, A, Okunola-Bakare, OM, Moore, M, Deschamps, JR, Rais, R, Slusher, BS, Newman, AH. Biorg. Med. Chem., 2015, 23, 4000-4012.
[34] Vass, M, Schmidt, É, Horti, F, Keserű, GM. Eur. J. Med. Chem., 2014, 77, 38-46.
[35] Nebel, N, Maschauer, S, Bartuschat, AL, Fehler, SK, Hübner, H, Gmeiner, P, Kuwert, T, Heinrich, MR, Prante, O, Hocke, C. Biorg. Med. Chem. Lett., 2014, 24, 5399-5403.
[36] Chen, J, Levant, B, Jiang, C, Keck, TM, Newman, AH, Wang, S. J. Med. Chem., 2014, 57, 4962-4968.
[37] Ananthan, S, Saini, SK, Zhou, G, Hobrath, JV, Padmalayam, I, Zhai, L, Bostwick, JR, Antonio, T, Reith, MEA, McDowell, S, Cho, E, McAleer, L, Taylor, M, Luedtke, RR. J. Med. Chem., 2014, 57, 7042-7060.
[38] Zajdel, P, Marciniec, K, Maślankiewicz, A, Grychowska, K, Satała, G, Duszyńska, B, Lenda, T, Siwek, A, Nowak, G, Partyka, A, Wróbel, D, Jastrzębska-Więsek, M, Bojarski, AJ, Wesołowska, A, Pawłowski, M. Eur. J. Med. Chem., 2013, 60, 42-50.
[39] Li, A, Mishra, Y, Malik, M, Wang, Q, Li, S, Taylor, M, Reichert, DE, Luedtke, RR, Mach, RH. Biorg. Med. Chem., 2013, 21, 2988-2998.
[40] Newman, AH, Beuming, T, Banala, AK, Donthamsetti, P, Pongetti, K, LaBounty, A, Levy, B, Cao, J, Michino, M, Luedtke, RR, Javitch, JA, Shi, L. J. Med. Chem., 2012, 55, 6689-6699.
[41] Johnson, M, Antonio, T, Reith, MEA, Dutta, AK. J. Med. Chem., 2012, 55, 5826-5840.
[42] Gogoi, S, Biswas, S, Modi, G, Antonio, T, Reith, MEA, Dutta, AK. ACS Med. Chem. Lett., 2012, 3, 991-996.
[43] Ye, N, Wu, Q, Zhu, L, Zheng, L, Gao, B, Zhen, X, Zhang, A. Biorg. Med. Chem., 2011, 19, 1999-2008.
[44] Tu, Z, Li, S, Cui, J, Xu, J, Taylor, M, Ho, D, Luedtke, RR, Mach, RH. J. Med. Chem., 2011, 54, 1555-1564.
[45] Ortega, R, Hübner, H, Gmeiner, P, Masaguer, CF. Biorg. Med. Chem. Lett., 2011, 21, 2670-2674.
[46] Levoin, N, Calmels, T, Krief, S, Danvy, D, Berrebi-Bertrand, I, Lecomte, J-M, Schwartz, J-C, Capet, M. ACS Med. Chem. Lett., 2011, 2, 293-297.
[47] Kortagere, S, Cheng, S-Y, Antonio, T, Zhen, J, Reith, MEA, Dutta, AK. Biochem. Pharmacol., 2011, 81, 157-163.
[48] Banala, AK, Levy, BA, Khatri, SS, Furman, CA, Roof, RA, Mishra, Y, Griffin, SA, Sibley, DR, Luedtke, RR, Newman, AH. J. Med. Chem., 2011, 54, 3581-3594.
[49] Gómez-Jeria, JS, Valdebenito-Gamboa, J. Der Pharma Chem., 2015, 7, 323-347.
[50] Gómez Jeria, JS. Boll. Chim. Farmac., 1982, 121, 619-625.
[51] Gómez-Jeria, JS. Int. J. Quant. Chem., 1983, 23, 1969-1972.
[52] Gómez-Jeria, JS, "Modeling the Drug-Receptor Interaction in Quantum Pharmacology," in *Molecules in Physics, Chemistry, and Biology*, J. Maruani Ed., vol. 4, pp. 215-231, Springer Netherlands, 1989.
[53] Gómez-Jeria, JS, Ojeda-Vergara, M. J. Chil. Chem. Soc., 2003, 48, 119-124.
[54] Gómez-Jeria, JS, *Elements of Molecular Electronic Pharmacology (in Spanish),* Ediciones Sokar, Santiago de Chile, 2013.
[55] Gómez-Jeria, JS. Canad. Chem. Trans., 2013, 1, 25-55.
[56] Fukui, K, Fujimoto, H, *Frontier orbitals and reaction paths: selected papers of Kenichi Fukui,* World Scientific, Singapore; River Edge, N.J., 1997.
[57] Frisch, MJ, Trucks, GW, Schlegel, HB, Scuseria, GE, Robb, MA, Cheeseman, JR, Montgomery, J, J.A., Vreven, T, Kudin, KN, Burant, JC, Millam, JM, Iyengar, SS, Tomasi, J, Barone, V, Mennucci, B, Cossi, M, Scalmani, G, Rega, N. G03 Rev. E.01, Gaussian, Pittsburgh, PA, USA, 2007.
[58] Gómez-Jeria, JS. D-Cent-QSAR: A program to generate Local Atomic Reactivity Indices from Gaussian 03 log files. 1.0, Santiago, Chile, 2014.
[59] Gómez-Jeria, JS. J. Chil. Chem. Soc., 2009, 54, 482-485.
[60] Statsoft. Statistica 8.0, 2300 East 14 th St. Tulsa, OK 74104, USA, 1984-2007.
[61] Joselevich, E. Ang. Chem. Int. Ed., 2004, 43, 2992-2994.
[62] Joselevich, E. ChemPhysChem, 2004, 5, 619-624.
[63] Hypercube. Hyperchem 7.01, 419 Phillip St., Waterloo, Ontario, Canada, 2002.
[64] Chemaxon. MarvinView, www.chemaxon.com, USA, 2014.
[65] Gómez-Jeria, JS, Morales-Lagos, D, Rodriguez-Gatica, JI, Saavedra-Aguilar, JC. Int. J. Quant. Chem., 1985, 28, 421-428.

[66] Gómez-Jeria, JS, Morales-Lagos, D, Cassels, BK, Saavedra-Aguilar, JC. Quant. Struct.-Relat., 1986, 5, 153-157.
[67] Gómez-Jeria, JS, Sotomayor, P. J. Mol. Struct. (Theochem), 1988, 166, 493-498.
[68] Gómez-Jeria, JS, Ojeda-Vergara, M, Donoso-Espinoza, C. Mol. Engn., 1995, 5, 391-401.
[69] Gómez-Jeria, JS, Ojeda-Vergara, M. Int. J. Quant. Chem., 1997, 61, 997-1002.
[70] Gómez-Jeria, JS, Lagos-Arancibia, L. Int. J. Quant. Chem., 1999, 71, 505-511.
[71] Gómez-Jeria, JS, Lagos-Arancibia, L, Sobarzo-Sánchez, E. Bol. Soc. Chil. Quím., 2003, 48, 61-66.
[72] Gómez-Jeria, JS, Soto-Morales, F, Larenas-Gutierrez, G. Ir. Int. J. Sci., 2003, 4, 151-164.
[73] Gómez-Jeria, JS, Gerli-Candia, LA, Hurtado, SM. J. Chil. Chem. Soc., 2004, 49, 307-312.
[74] Gómez-Jeria, JS, Soto-Morales, F, Rivas, J, Sotomayor, A. J. Chil. Chem. Soc., 2008, 53, 1393-1399.
[75] Gómez-Jeria, JS. J. Chil. Chem. Soc., 2010, 55, 381-384.
[76] Bruna-Larenas, T, Gómez-Jeria, JS. Int. J. Med. Chem., 2012, 2012 Article ID 682495, 1-16.
[77] Gómez-Jeria, JS. Der Pharm. Lett., 2014, 6., 95-104.
[78] Gómez-Jeria, JS. SOP Trans. Phys. Chem., 2014, 1, 10-28.
[79] Gómez-Jeria, JS. J. Comput. Methods Drug Des., 2014, 4, 32-44.
[80] Gómez-Jeria, JS, Molina-Hidalgo, J. J. Comput. Methods Drug Des., 2014, 4, 1-9.
[81] Gómez-Jeria, JS, Valdebenito-Gamboa, J. Der Pharma Chem., 2014, 6, 383-406.
[82] Salgado-Valdés, F, Gómez-Jeria, JS. J. Quant. Chem., 2014, 2014 Article ID 431432, 1-15.
[83] Solís-Gutiérrez, R, Gómez-Jeria, JS. Res. J. Pharmac. Biol. Chem. Sci., 2014, 5, 1401-1416.
[84] Gómez-Jeria, JS, Reyes-Díaz, I, Valdebenito-Gamboa, J. J. Comput. Methods Drug Des., 2015, 5, 25-56.
[85] Gómez-Jeria, JS, Robles-Navarro, A. Der Pharma Chem., 2015, 7, 243-269.
[86] Gómez-Jeria, JS, Robles-Navarro, A. Res. J. Pharmac. Biol. Chem. Sci., 2015, 6, 1811-1841.
[87] Gómez-Jeria, JS, Robles-Navarro, A. Res. J. Pharmac. Biol. Chem. Sci., 2015, 6, 1358-1373.
[88] Leal, MS, Robles-Navarro, A, Gómez-Jeria, JS. Der Pharm. Lett., 2015, 7, 54-66.